

# The anion conductance of the glutamate transporter EAAC1 depends on the direction of glutamate transport

Natalie Watzke, Christof Grewer\*

Max-Planck-Institut für Biophysik, Kennedyallee 70, D-60596 Frankfurt, Germany

Received 31 May 2001; accepted 10 July 2001

First published online 26 July 2001

Edited by Maurice Montal

**Abstract** The steady-state and pre-steady-state kinetics of glutamate transport by the neuronal glutamate transporter EAAC1 were determined under conditions of outward glutamate transport and compared to those found for the inward transport mode. In both transport modes, the glutamate-induced current is composed of two components, the coupled transport current and the uncoupled anion current, and inhibited by a specific non-transportable inhibitor. Furthermore, the glutamate-independent leak current is observed in both transport modes. Upon a glutamate concentration jump outward transport currents show a distinct transient phase that deactivates within 15 ms. The results demonstrate that the general properties of EAAC1 are symmetric, but the rates of substrate transport and anion flux are asymmetric with respect to the orientation of the substrate binding site in the membrane. Therefore, the EAAC1 anion conductance differs from normal ligand-gated ion channels in that it can be activated by glutamate and  $\text{Na}^+$  from both sides of the membrane. © 2001 Federation of European Biochemical Societies. Published by Elsevier Science B.V. All rights reserved.

**Key words:** Glutamate transporter; Reverse transport; DL-threo- $\beta$ -Benzyloxyaspartate; Rapid kinetics

## 1. Introduction

In the mammalian brain, L-glutamate is the major excitatory neurotransmitter [1]. It is responsible for chemical signal transmission at the synapse and leads in high concentrations to excitotoxicity [2]. Glutamate is removed from the synapse by active uptake mediated by high affinity plasma membrane glutamate transporters. In order to maintain a  $10^6$ -fold concentration gradient of glutamate across the membrane, the uptake of one glutamate molecule is coupled to the co-transport of three sodium ions, one proton and the countertransport of one potassium ion [3]. In addition to their transporter function, glutamate transporters are associated with an anion conductance [4–7], which shows glutamate-dependent and glutamate-independent components, but strictly requires the presence of  $\text{Na}^+$  [5,8,9].

Under pathophysiological conditions, such as energy deprivation or ischemia, glutamate transporters catalyze the efflux of glutamate from the cytosol of glial and neuronal cells into the synaptic cleft [10,11], although the affinity for glutamate on the intracellular side is 40-fold lower compared to the

extracellular side [12]. However, apart from the apparent affinity of EAAC1 for glutamate not much is known about the thermodynamic and kinetic properties of glutamate transporters in the outward transport mode. Therefore, we focused in this work on the investigation of the neuronal glutamate transporter subtype EAAC1 (excitatory amino acid carrier 1) under outward transport conditions and compared the results to those obtained for the inward transport mode in order to test whether EAAC1 operates symmetrically. Some of the important questions that are addressed here are: (i) Do non-transportable inhibitors bind to the intracellular side of EAAC1? (ii) Can the glutamate-induced and the leak anion conductance be activated by applying substrates to the intracellular side of EAAC1? (iii) Is it possible to detect pre-steady-state transient currents in the outward transport mode? To answer these questions we used a combined approach of current recording from EAAC1 expressing cells together with a rapid chemical kinetic technique to apply glutamate to the intracellular side of EAAC1 within 100  $\mu\text{s}$  [8,12].

## 2. Materials and methods

### 2.1. Expression and electrophysiological recording

Rat EAAC1 cDNA [13] was used for transient transfection of sub-confluent human embryonic kidney cell (HEK293, ATCC No. CGL 1573) cultures with the calcium phosphate-mediated transfection method [14] as described [8]. Electrophysiological recordings were performed 24 h after transfection for 3 days with an Adams and List EPC7 amplifier under voltage-clamp conditions in the inside-out and whole-cell current recording configuration [15]. The typical resistance of the recording electrode was 300–400 k $\Omega$  (patch) or 2–3 M $\Omega$  (whole cell). Recording solutions: pipet solutions (in mM) 130 KSCN or KCl, 2 MgCl<sub>2</sub>, 10 TEACl, 10 EGTA and 10 HEPES (pH 7.4/KOH); bath solutions (in mM) 140 NaCl or NaSCN, 2 MgCl<sub>2</sub>, 2 CaCl<sub>2</sub>, 30 HEPES (pH 7.4/NaOH). The blocker DL-threo- $\beta$ -benzyloxyaspartate (TBOA) was obtained from Tocris (Bristol, UK). All the experiments were performed at room temperature and repeated at least five times with at least two different patches/cells. The error bars represent the error of a single measurement (mean  $\pm$  S.D.).

### 2.2. Laser-pulse photolysis and solution exchange

Solution exchange was performed by means of a quartz tube (opening 350  $\mu\text{m}$ ) positioned at a distance of  $\approx 0.5$  mm from the cell. The flow velocity of the solutions emerging from the opening of the tube was approx. 5–10 cm/s. Laser-pulse photolysis experiments were performed as described previously [16].  $\alpha\text{CNB}$ -caged glutamate (Molecular Probes) in concentrations of  $\leq 6$  mM or free glutamate were applied to the cells and photolysis of the caged glutamate was initiated with a light flash (500–840 mJ/cm<sup>2</sup>, 340 nm, 15 ns, excimer laser pumped dye laser, Lambda Physik, Göttingen, Germany). The light was coupled to a quartz fiber (diameter 365  $\mu\text{m}$ ) that was positioned

\*Corresponding author. Fax: (49)-69-6303 305.  
E-mail address: grewer@mpibp-frankfurt.mpg.de (C. Grewer).

in front of the cell at a distance of 300  $\mu\text{m}$ . The released glutamate concentration was estimated by comparison of the steady-state current with that generated by rapid perfusion of the same cell or patch with 0.1 mM or 5 mM glutamate [17].

Data were recorded using the pClamp6 software (Axon Instruments, Foster City, CA, USA), digitized with a sampling rate of 1 kHz (solution exchange) or 25 kHz (laser-pulse photolysis) and low pass-filtered at 250 Hz or 3 kHz, respectively.

### 3. Results and discussion

Electrophysiological experiments on EAAC1 in the inward transport mode revealed three individual EAAC1-associated currents: the  $\text{Na}^+/\text{K}^+$ -coupled glutamate transport current  $I_{\text{Na}^+/\text{K}^+}^{\text{Glu}^-}$ , the glutamate-induced uncoupled anion current  $I_{\text{anionic}}^{\text{Glu}^-}$  and the glutamate-independent leak anion current  $I_{\text{anionic}}$  [8,18]. All three EAAC1-associated currents can be inhibited by the competitive blocker TBOA [8]. The experiments described below compare these different current components of glutamate transporters in the inward transport mode with those found in the outward transport mode.

#### 3.1. Symmetry of glutamate-induced transport and anion currents

First, we determined the relationship between the glutamate transport current  $I_{\text{Na}^+/\text{K}^+}^{\text{Glu}^-}$  and the glutamate-induced anion current  $I_{\text{anionic}}^{\text{Glu}^-}$  for EAAC1 in the inward transport mode. Whole-cell current recordings on HEK<sub>EAAC1</sub> cells were performed with a chloride-based pipet solution (intracellular). The application of a saturating concentration of glutamate (125  $\mu\text{M}$ ) in a chloride-based bath solution (extracellular) leads to an inward current as shown in Fig. 1A. Under these conditions and with 0 mV transmembrane potential only  $I_{\text{Na}^+/\text{K}^+}^{\text{Glu}^-}$  is observed, which is associated with the movement of two positive charges into the cell. In contrast, the application of glutamate in a  $\text{SCN}^-$ -based bath solution on the same cell resulted in a current in the opposite direction (Fig. 1A). Since EAAC1 is quite permeable for  $\text{SCN}^-$ ,  $I_{\text{Na}^+/\text{K}^+}^{\text{Glu}^-}$  is now superimposed by the glutamate-induced anion current  $I_{\text{anionic}}^{\text{Glu}^-}$ , which is outwardly directed ( $\text{SCN}^-$  influx). The ratio between  $I_{\text{Na}^+/\text{K}^+}^{\text{Glu}^-}$  and  $I_{\text{anionic}}^{\text{Glu}^-}$  is 1:(3.7  $\pm$  0.7) (Fig. 1C). This result demonstrates that approximately eight  $\text{SCN}^-$  ions move across the membrane in one EAAC1 transport cycle, under these conditions. The same experiment was repeated on inside-out patches for EAAC1 in the outward transport mode (Fig. 1B). Here, the application of a saturating concentration of glutamate [12] leads to a positive transport current  $I_{\text{Na}^+/\text{K}^+}^{\text{Glu}^-}$ , since the outward transport of glutamate is associated with the movement of positive charge from the intracellular to the extracellular side. After replacing intracellular  $\text{Cl}^-$  with  $\text{SCN}^-$  the glutamate-induced current was inwardly directed, showing that outward movement of  $\text{SCN}^-$  generates a current in the opposite direction compared to the glutamate transport current. For EAAC1 in the outward transport mode the ratio between  $I_{\text{Na}^+/\text{K}^+}^{\text{Glu}^-}$  and  $I_{\text{anionic}}^{\text{Glu}^-}$  is 1:(1.45  $\pm$  0.1) (Fig. 1C). These findings directly demonstrate that (i) the glutamate-dependent anion conductance can be evoked by application of glutamate to the intracellular side of EAAC1, as was previously proposed for glial glutamate transporters in Müller cells [19] and is shown schematically in Fig. 3B, and (ii) in the outward transport mode the anion current contributes to the glutamate-induced signal to a smaller extent compared to EAAC1 in the inward transport mode.

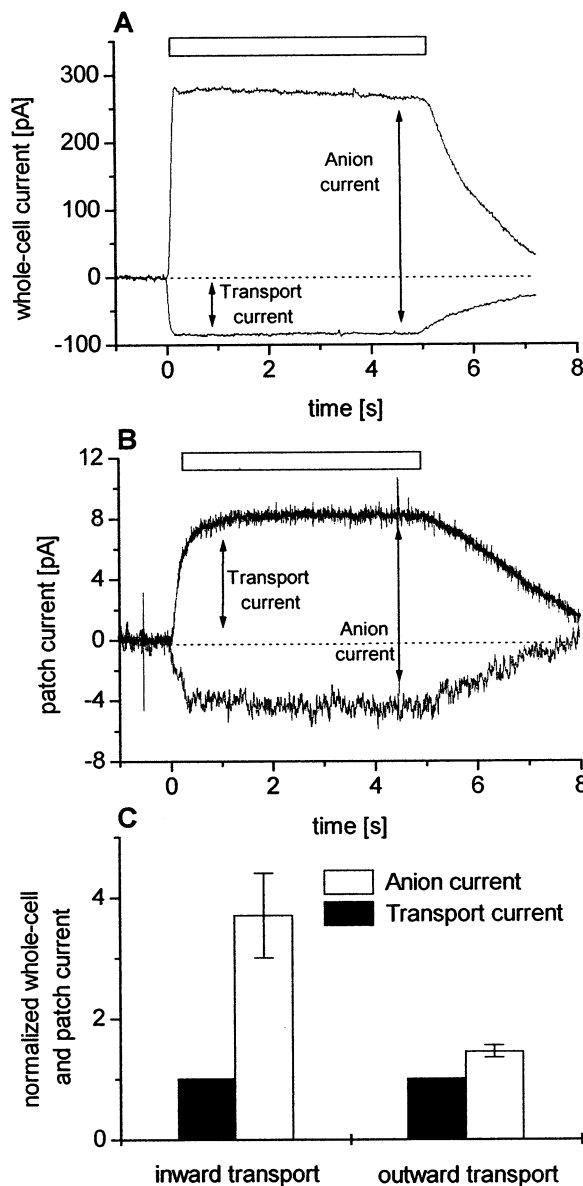


Fig. 1. A: Whole-cell current recordings of an EAAC1 expressing HEK293 cell upon rapid application of 125  $\mu\text{M}$  glutamate (indicated by the bar) preincubated in a NaSCN-based (upper trace) or NaCl-based (lower trace) bath solution (KCl-based pipet solution, 0 mV transmembrane potential). Leak currents were subtracted. B: Same conditions as in A on an inside-out HEK<sub>EAAC1</sub> patch with the application of 5 mM glutamate. The lower trace (NaSCN-based bath solution) was low-pass filtered at 40 Hz. C: Relative magnitude of  $I_{\text{anionic}}^{\text{Glu}^-}$  and  $I_{\text{Na}^+/\text{K}^+}^{\text{Glu}^-}$  for EAAC1 in the inward and the outward transport mode ( $n = 4-6$ ).

#### 3.2. EAAC1 is inhibited by TBOA in the outward transport mode

We then asked the question whether the glutamate-induced current of EAAC1 in the outward transport mode can be blocked by the competitive inhibitor TBOA, as reported for EAAC1 in the inward transport mode [8,20]. To test this, a nearly half-saturating concentration (0.2 mM) of glutamate [12] was applied to inside-out excised membrane patches. The additional application of TBOA resulted in an inhibition of the glutamate-induced current with an apparent  $K_i$  value for TBOA of 150  $\pm$  20  $\mu\text{M}$  (Fig. 2A). Thus (i) TBOA is a blocker on the intracellular side of EAAC1 and (ii) the intra-

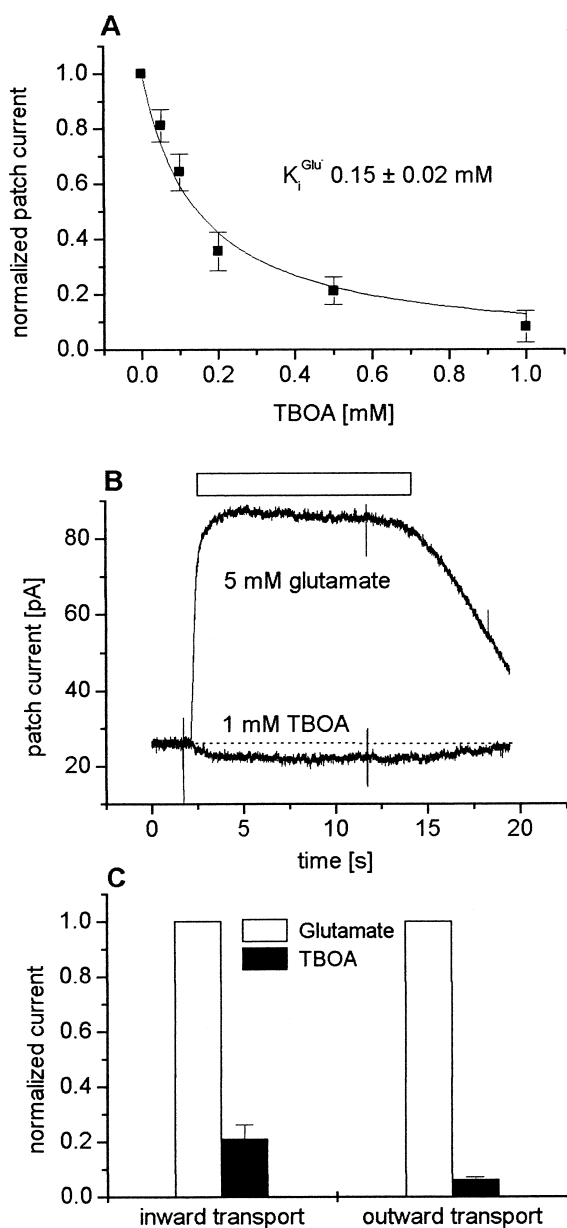


Fig. 2. A: Determination of the apparent  $K_i$  value for TBOA in the presence of 0.2 mM glutamate and a holding potential of 0 mV on inside-out HEK<sub>EAAC1</sub> patches. The data were fitted with the function  $I = K_i / (K_i + [TBOA])$ , with  $K_i = 0.15 \pm 0.02$  mM (solid line). B: Inside-out patch recording from a HEK<sub>EAAC1</sub> cell upon application of 5 mM glutamate (upper trace) or 1 mM TBOA (lower trace). The transmembrane potential was set to 0 mV, KSCN-based pipet solution. C: Relative magnitudes of glutamate-induced and TBOA-induced whole-cell currents (inward transport) or inside-out patch currents (outward transport) ( $n = 2-5$ ).

cellular binding site of TBOA has an approx. 100–200-fold lower affinity than the one located on the extracellular side of EAAC1. A qualitatively similar effect was found previously for the binding of glutamate to EAAC1 by comparing its apparent dissociation constant in the inward and outward transport mode [12].

### 3.3. Glutamate-independent anion conductance

For EAAC1 in the inward transport mode it was shown

that TBOA inhibits the glutamate-independent leak anion current  $I_{\text{anionic}}$  [8,9]. Under these conditions the application of TBOA to the extracellular side of EAAC1 in the presence of intracellular  $\text{SCN}^-$  and the absence of glutamate leads to an outward current, caused by inhibiting the continuous efflux of  $\text{SCN}^-$  ( $I_{\text{anionic}}$ ). The same experiment was repeated for EAAC1 in the outward transport mode by applying TBOA from the intracellular side and with  $\text{SCN}^-$  on the extracellular side (pipet solution). As shown in Fig. 2B, a small but significant inward current was detected ( $n = 2$ ). The amplitude of the TBOA-induced current showed no difference when either 1 mM or 2 mM TBOA was applied, indicating that these concentrations are saturating the TBOA binding site on EAAC1. The ratio between the glutamate-induced current (5 mM) and the TBOA-induced current was 1:( $0.05 \pm 0.01$ ) for EAAC1 in the outward transport mode and 1:( $0.21 \pm 0.05$ ) for EAAC1 in the inward transport mode (Fig. 2C). These results demonstrate that (i)  $I_{\text{anionic}}$  can be carried by EAAC1 under conditions that favor outward transport (see Fig. 3B) and (ii) the leak anion conducting state in the absence of glutamate seems to be less populated under outward transport than under inward transport conditions, similar to our findings for the glutamate-dependent component of the anion conductance.

### 3.4. Time-resolved measurements on EAAC1 in the outward transport mode

The onset of the current of EAAC1 evoked by rapid solution exchange in the inside-out patch configuration is relatively slow with rise times in the 100 ms-to-second range, even when applying supersaturating concentrations of glutamate, as shown in Fig. 2B. This is caused most likely by the fact that the patch membrane is invaginated into the pipet. Thus the  $\Omega$  shape of the inside-out patches reduces the high time resolution [21], which can be achieved with outside-out patches as demonstrated by Otis and Kavanaugh [18]. With the laser-pulse photolysis technique and using  $\alpha\text{CNB}$ -caged glutamate as an inert photolabile glutamate precursor [8,12] it was possible to circumvent this problem. Upon a glutamate concentration jump to 1.5–1.8 mM a transient current component preceding the stationary current was resolved, as shown in Fig. 3A. The observed time constants are  $0.5 \pm 0.1$  ms for the current rise and  $4.4 \pm 1.0$  ms ( $n = 2$ ) for the current decay in the presence of extracellular  $\text{SCN}^-$  (the current reflects a sum of  $I_{\text{Na}^+/\text{K}^+}^{\text{Glu}^-}$  and  $I_{\text{anionic}}^{\text{Glu}^-}$ ). In addition, we observed a slow component of the current decay, but since the amplitude of this second phase was small ( $\approx 12\%$  of the total current) it was not evaluated quantitatively. Similar transient currents were observed in the inward transport mode with time constants in the presence of  $\text{SCN}^-$  in the range of  $0.8 \pm 0.1$  ms for the current rise and  $9.4 \pm 0.9$  ms ( $n = 10$ ) for the current decay (Fig. 3). Thus the time constants determined for EAAC1 in the outward transport mode are about half of the time constants for EAAC1 in the inward transport mode and resemble more the kinetics of the coupled transport component current measured in the absence of  $\text{SCN}^-$  [8]. This difference may be due to the fact that in the outward transport mode the transport current contributes to a larger extent to the glutamate-induced current than in the inward transport mode (Fig. 1C). The observation of a pre-steady-state transient current suggests in both the outward and the inward transport mode the existence of short-lived transporter reac-

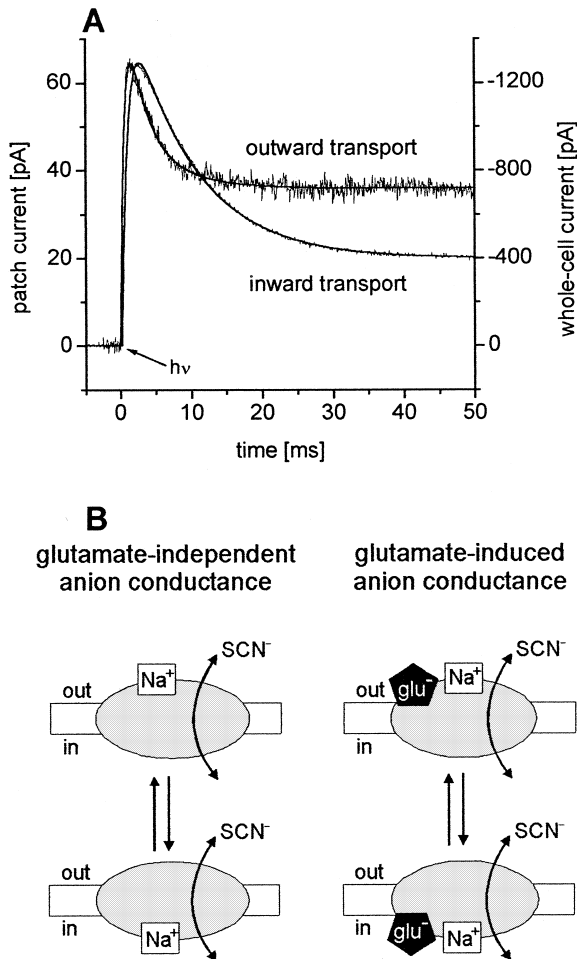


Fig. 3. A: Laser-pulse photolysis experiments on EAAC1 in the outward transport mode (inside-out patch) and in the inward transport mode (whole-cell current recording) with a KSCN-based pipet solution, NaCl-based bath solution and a transmembrane potential of 0 mV. The current traces were fitted with the following function:  $I = I_1 \exp(-t/\tau_{\text{decay}}) + I_2 \exp(-t/\tau_{\text{rise}}) + I_{\text{ss}}$ . The parameters for outward transport were: 6 mM caged glutamate  $\approx$  1.8 mM free glutamate,  $\tau_{\text{rise}} = 0.4 \pm 0.1$  ms and  $\tau_{\text{decay}} = 4.8 \pm 0.1$  ms; inward transport: 1 mM caged glutamate  $\approx$  150  $\mu$ M free glutamate,  $\tau_{\text{rise}} = 0.9 \pm 0.1$  ms and  $\tau_{\text{decay}} = 9.5 \pm 0.1$  ms. B: Hypothetical mechanism for the glutamate-independent leak anion conductance and the glutamate-induced anion conductance for EAAC1 in the glutamate inward and outward transport mode. The exact number of bound sodium ions required for activating the anion conducting modes is not precisely known [9] and is, therefore, not specified in the mechanism shown here.

tion intermediates. These transiently populated intermediates precede steady-state turnover of EAAC1.

### 3.5. Conclusions

We reported here that EAAC1, under conditions of outward transport, displays all three EAAC1-associated current components: the glutamate transport current  $I_{\text{Na}^+/\text{K}^+}^{\text{Glu}^-}$  and both anion conducting activities  $I_{\text{anionic}}^{\text{Glu}^-}$  and  $I_{\text{anionic}}$ , as was previously shown for EAAC1 in the inward transport mode [8,18]. Thus, the general mechanism of operation of EAAC1 is symmetric with respect to the plane of the membrane, as illustrated in Fig. 3B. These findings suggest that the behavior of the glutamate-gated anion conductance of EAAC1 is more

reversible transporter-like than ligand-gated ion channel-like, since the latter channels are typically asymmetrically ligand-gated from only one side of the membrane. The fact that TBOA blocks both the glutamate-induced and the glutamate-independent currents implies that TBOA, which is a potent blocker of inward glutamate transport [22], also interacts with the glutamate binding site on the intracellular side of EAAC1. Thus the geometry and specificity of the glutamate binding site exposed to the cytosol appears to be quite similar to that exposed to the extracellular side. This finding is consistent with typical alternating access models of secondary transport, in which the same binding site for the organic substrate and co-transported ions can be exposed to either side of the membrane, depending on the conformation of the transporter. The thermodynamic apparent constants of substrate and inhibitor binding as well as the kinetic constants for pre-steady-state reaction steps, however, are asymmetric. For example the 40-fold change in affinity of EAAC1 for binding of glutamate to its intracellular site is mainly caused by changes of equilibrium constants of other reactions under steady-state conditions, such as proton binding to EAAC1 [12]. A similar mechanism may hold for the affinity shift found for TBOA. This asymmetry may also be responsible for the lower population of the glutamate-dependent and glutamate-independent anion conducting states and the change in pre-steady-state kinetics of EAAC1 under outward transport conditions. Finally, it is important to note that the results presented here suggest that it will be possible to develop pharmacologically active compounds that act on the intracellular glutamate binding site of EAAC1 to prevent efflux of excitotoxic glutamate under conditions of energy deprivation and, thus, to alleviate the nerve damaging effects associated with it.

**Acknowledgements:** We thank T. Rauen for kindly providing EAAC1 cDNA, E. Bamberg for continuous encouragement and support and E. Bamberg and K. Fendler for critical reading of the manuscript. This work was supported by the Deutsche Forschungsgemeinschaft (grant 1393/2-1 awarded to C.G.).

### References

- [1] Kandel, E.R., Schwartz, J.H. and Jessell, T.M. (1995) *Principals of Neutral Science*, Appleton and Lange.
- [2] Choi, D.W. (1988) *Neuron* 1, 623–634.
- [3] Zerangue, N. and Kavanaugh, M.P. (1996) *Nature* 383, 634–637.
- [4] Fairman, W.A., Vandenberg, R.J., Arriza, J.L., Kavanaugh, M.P. and Amara, S.G. (1995) *Nature* 375, 599–603.
- [5] Otis, T.S. and Jahr, C.E. (1998) *J. Neurosci.* 18, 7099–7110.
- [6] Wadiche, J.I., Amara, S.G. and Kavanaugh, M.P. (1995) *Neuron* 15, 721–728.
- [7] Wadiche, J.I. and Kavanaugh, M.P. (1998) *J. Neurosci.* 18, 7650–7661.
- [8] Grewer, C., Watzke, N., Wiessner, M. and Rauen, T. (2000) *Proc. Natl. Acad. Sci. USA* 97, 9706–9711.
- [9] Watzke, N., Bamberg, E. and Grewer, C. (2001) *J. Gen. Physiol.* 117, 547–562.
- [10] Jabaudon, D., Scanziani, M., Gahwiler, B.H. and Gerber, U. (2000) *Proc. Natl. Acad. Sci. USA* 97, 5610–5615.
- [11] Rossi, D.J., Oshima, T. and Attwell, D. (2000) *Nature* 403, 316–321.
- [12] Watzke, N., Rauen, T., Bamberg, E. and Grewer, C. (2000) *J. Gen. Physiol.* 116, 609–621.
- [13] Rauen, T., Rothstein, J.D. and Wassele, H. (1996) *Cell Tissue Res.* 286, 325–336.
- [14] Chen, C. and Okayama, H. (1987) *Mol. Cell. Biol.* 7, 2745–2752.
- [15] Hamill, O.P., Marty, A., Neher, E., Sakmann, B. and Sigworth, F.J. (1981) *Pflug. Arch. Eur. J. Physiol.* 391, 85–100.

- [16] Niu, L., Grewer, C. and Hess, G.P. (1996) in: *Techniques in Protein Chemistry VII* (Marshak, D.R., Ed.), Academic Press, New York.
- [17] Grewer, C. (1999) *Biophys. J.* 77, 727–738.
- [18] Otis, T.S. and Kavanaugh, M.P. (2000) *J. Neurosci.* 20, 2749–2757.
- [19] Billups, B., Rossi, D. and Attwell, D. (1996) *J. Neurosci.* 16, 6722–6731.
- [20] Shimamoto, K., Shigeri, Y., Yasuda-Kamatani, Y., Lebrun, B., Yumoto, N. and Nakajima, T. (2000) *Bioorg. Med. Chem.* 10, 2407–2410.
- [21] Jonas, P. (1995) in: *Single-Channel Recording* (Sakmann, B. and Neher, E., Eds.), pp. 231–243, Plenum Press, New York.
- [22] Lebrun, B., Sakaitani, M., Shimamoto, K., Yasuda-Kamatani, Y. and Nakajima, T. (1997) *J. Biol. Chem.* 272, 20336–20339.